August 27-31, 2023
FLORENCE - ITALY
16th International Conference on Wind Engineering

Characteristics of wind speed profiles through numerical studies of Super Typhoon Lekima (2019)

Tiantian Li [1], Shengming Tang [1], Yongping Li [1]

[1]*Shanghai Typhoon Institute of China Meteorological Administration, Shanghai, China, litt@typhoon.org.cn*

SUMMARY:
Rapid growth in global wind energy industry and significant expansion in offshore wind market have led to the development of bigger and higher wind turbines (exceeding 200 m). The traditional similarity theory of turbulence, which is the basis of current wind turbine design theory and wind energy resource assessment, may not be applicable, since it assumes a constant flux in the surface layer of about 100 m high. In the study, Computational Fluid Dynamics (CFD) simulations based on large eddy simulation (LES) method were conducted to further understand wind speed profiles under complex terrain during typhoons, which were improved and validated by field experiments. The results showed that power-law profile can describe wind speeds below 100 m well, but is less effective for wind speeds below 300 m because of local reverses or low-level jets. Besides, there is a negative linear correlation between terrain elevation and power exponents of fitted wind speed profiles. The study provides useful information to better understand characteristics of typhoon-induced wind speed profiles in the boundary layer concentrated between 100 and 300 m, facilitating typhoon-resistant design of large-scale wind turbines and wind energy assessment.

Keywords: wind speed profile, typhoon, complex terrain

1. INTRODUCTION

In recent years, global wind energy industry has grown rapidly and offshore wind market has expanded significantly. According to Global Wind Energy Council (GWEC, 2022), 93.6 GW of new wind power capacity was added worldwide in 2021, surpassing 90 GW for two consecutive years. Such rapid growth is resulted from bigger and higher wind turbines. For example, the single-unit capacity of wind turbines has leaped from tens of kilowatts in the early days to ten megawatts today, and the tip height of wind turbines has already exceeded 200 m. However, current wind turbine design theory and wind energy resource assessment are still based on the similarity theory of turbulence (Monin and Obukhov, 1954). Since it assumes the vertical stress distribution is nearly constant in the layer near the surface, it is mainly applicable to a height of about 100 m above ground. This may cause potential safety issues for risk analysis of big wind turbines and less accurate assessment of wind energy resources. To solve this problem, current study intends to apply Computational Fluid Dynamics (CFD) simulations to help analyse wind speed profiles at a height between 0-300 m. Considering the development of offshore wind turbines and threats posed by typhoon-induced extreme winds at coastal and nearshore regions, current study is focused on analysis of typhoon-induced wind speed profiles under complex terrain.

2. OVERVIEW OF SUPER TYPHOON LEKIMA (2019)

The typhoon selected in the study is Super Typhoon Lekima, which is the ninth named tropical cyclone of the 2019 Pacific typhoon season. Lekima made landfall on the coast of Chengnan of Zhejiang Province (China) at 01:45 CST on August 10. At the time of landing, the maximum wind speed near the centre was 52 m/s, and the minimum central pressure was 930 hPa. Field experiments were performed at Sansha Observatory in Fujian Province, as indicated by red square in Fig. 1. Doppler wind lidar (DWL) and wind tower equipped with ultrasonic anemometers observations were made, and the data were used for CFD simulations.

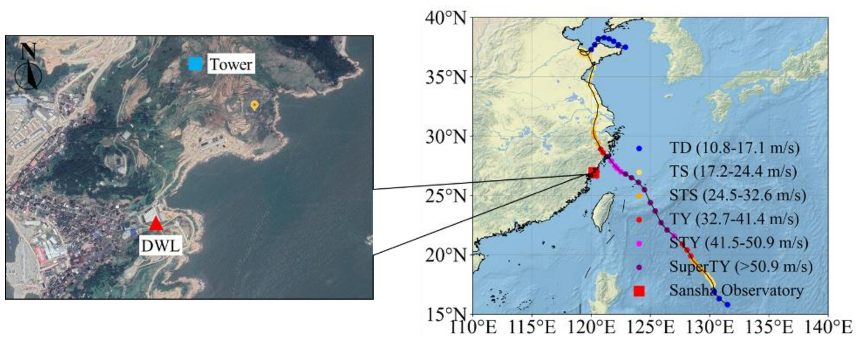

Figure 1. Best track of Super Typhoon Lekima (2019) and location of Sansha Observatory.

3. NUMERICAL STUDY

CFD simulation of Sansha Observatory is conducted through commercial software Fluent 19.2. The established numerical model is presented in Fig.2. From Figs.2(a-b), velocity inlet, pressure outlet, no-slip wall, and symmetry boundary conditions are applied for the numerical model. Mesh arrangement of the model is presented in Fig.2(c), and height of the first layer of cell is 0.02 m. In total, 2.35 million cells are generated. The input at velocity inlet is determined based on DWL observations, and the equilibrium inflow boundary condition based on RANS equations (Yang et al., 2009) is also applied to maintain the equilibrium of wind field from inlet to outlet. The finally determined velocity input is given in Eq. (1). Large eddy simulation (LES) is selected for turbulence modelling, with dynamic Smagorinsky-Lilly model as the subgrid-scale model. Semi-implicit method for pressure linked equation consistent (SIMPLEC) is adopted to solve the governing equations.

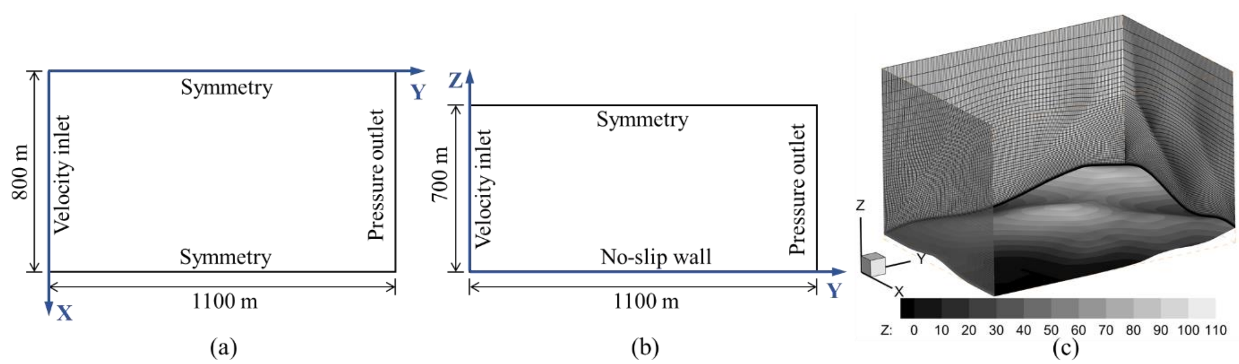

Figure 2. Numerical model: (a) Top view; (b) front view; (c) mesh arrangement (ground is shaded by z-coordinates).

$$u(z) = \frac{0.4205}{\kappa} \ln\left(\frac{z+0.08}{0.08}\right) \quad (1a)$$

$$k(z) = \sqrt{-0.9858 \cdot \ln(z + 0.08) + 6.555} \quad (1b)$$

$$\omega(z) = C_\mu^{-1/2} \frac{\partial u(z)}{\partial z} \quad (1c)$$

where $u(z)$ is wind speed profile; z is the height above ground; κ is von Kármán's constant, taken as 0.4; $k(z)$ is the profile of turbulent kinetic energy; $\omega(z)$ is the profile of specific dissipation rate; C_μ is model constant, taken as 0.09.

CFD simulation results are validated based on wind tower observations in Sansha Observatory, which are in general agreement with wind tower data. Mean wind speed profiles averaging from LES simulations are presented in Fig. 3. In the uphill direction (Fig. 3c), six wind speed profiles are extracted, which are located at 100, 200, 300, 400, 500, and 620 m far away from the velocity inlet. In general, wind speed increases with the increase of terrain elevation. Wind speed also increases with height except for the wind speed profile at the highest elevation (Distance=620 m) where a completely reversed and almost monotonically decreasing profile is found. For the wind speed profiles in the downhill direction (Fig. 3d), which are located at 620, 700, 800, 900, and 1000 m far away from the inlet, wind speed decreases with the decrease of terrain elevation. The reversed wind speed profile is also found at the distance of 700 m.

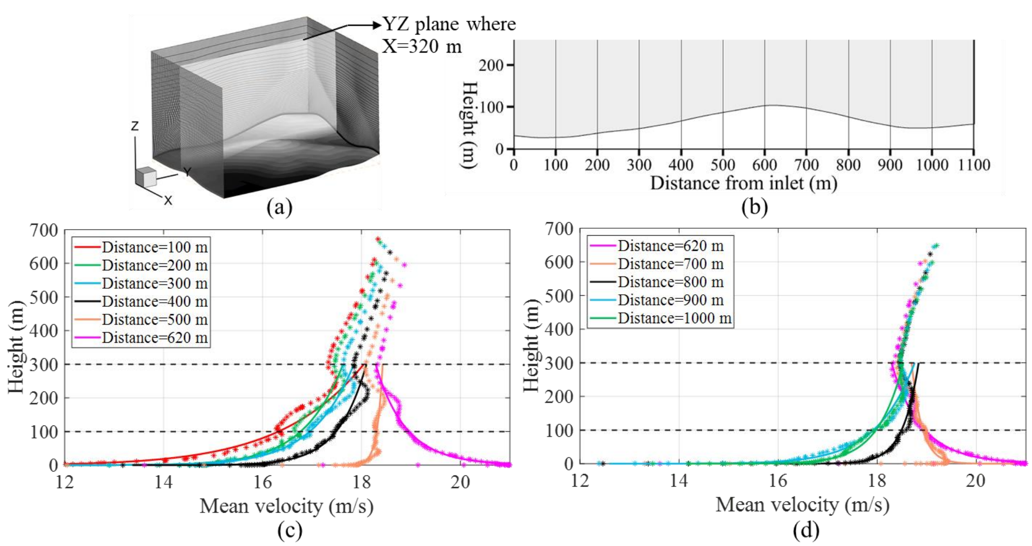

Figure 3. (a) Indication of YZ plane where X=320 m; (b) Illustration of terrain elevations at YZ plane where X=320 m; Comparisons between simulated results (dotted star) and fitted power-law profiles (solid line) for (c) uphill and (d) downhill.

Power-law profile is used to fit wind speeds along height from numerical simulations. Wind speeds below 100 m are first used to do regression analysis. Simulated wind speed profiles, excepting those at 500 and 700 m, generally agree with power-law profile, with R^2 of all regression lines greater than 0.96, maximum mean error of 0.19 m/s and maximum root-mean-square error of 0.23 m/s. Since wind speed profiles at 500 and 700 m are located in such region where wind speed profile transitions from monotonically increasing to monotonically decreasing, wind speed profiles endure more oscillations. Therefore, wind speed profiles cannot be well described by the power law and the error is relatively larger. The power-law regression is then applied to wind speeds below 300 m (Figs. 3c-d). Wind speed profiles no longer increase or decrease monotonically. Local reverses are observed at heights between 110-130 m and low-level jets at 180-250 m for uphill. For downhill, jets normally occur at a height of 220 m. In such case, the power law is less effective. Qualitatively, R^2 is decreased by 0.11 and mean error is increased by 0.08 m/s when compared to regression analysis of wind speeds below 100 m.

In addition, power exponents of fitted wind speed profiles between 0-100 m and 0-300 m are correlated to terrain elevations, and a linear relation is found, which are characterized and presented in Fig. 4. Power exponents decrease with increasing terrain elevation, and become negative at higher elevation, corresponding to reversed wind speed profiles. For power exponents $\alpha_{100\text{m}}$ and $\alpha_{300\text{m}}$, $\alpha_{300\text{m}}$ is larger than $\alpha_{100\text{m}}$ when terrain elevation is lower than 80 m, and vice versa.

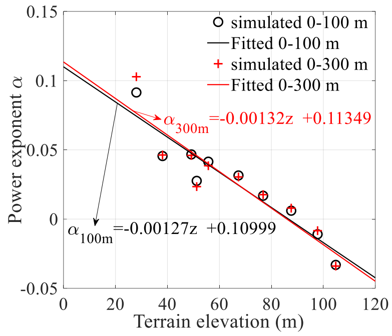

Figure 4. Linear relation between power exponents and terrain elevations.

4. CONCLUSIONS

From the numerical study, power-law profile is able to characterize wind speeds below 100 m, with positive exponent in the uphill/downhill direction and negative one at the highest elevation. For wind speeds below 300 m, the appearance of local reverses or low-level jets leads to oscillated profiles and power-law profile is less effective, with R^2 of regression lines reducing by 0.11 compared to the one below 100 m. Besides, a negative linear correlation between power exponents of fitted wind speed profiles and terrain elevations is established. The above findings are useful to better understand characteristics of typhoon-induced wind speed profiles in the boundary layer concentrated between 100 and 300 m, facilitating typhoon-resistant design of bigger and higher wind turbines and accurate assessment of wind energy resources.

ACKNOWLEDGEMENTS

This work was supported by the National Natural Science Foundation of China (Nos. 42005144, U2142206); China Postdoctoral Science Foundation (No. 2020M681443); Shanghai Postdoctoral Excellence Program (No. 2020518); Basic Research Fund of Shanghai Typhoon Institute (No. 2022JB01).

REFERENCES

GWEC (Global Wind Energy Council). Global Wind Report 2022.

Monin, A. S. and Obukhov, A. M., 1954. Basic laws of turbulent mixing in the surface layer of the atmosphere. Tr. Akad. Nauk SSSR Geophiz. Inst. 24(151): 163–187.

Yang, Y., Gu, M., Chen, S. and Jin, X., 2009. New inflow boundary conditions for modelling the neutral equilibrium atmospheric boundary layer in computational wind engineering. Journal of Wind Engineering and Industrial Aerodynamics 97(2), 88–95.